Retraction

Retracted: Effect of Orthodontic Combined with Implant Repair on Aesthetic Effect and Gingival Crevicular Fluid Factor in Patients with Dentition Defect and Periodontitis

BioMed Research International

This article has been retracted by Hindawi following an investigation undertaken by the publisher [1]. This investigation has uncovered evidence of one or more of the following indicators of systematic manipulation of the publication process:

(1) Discrepancies in scope

(2) Discrepancies in the description of the research reported

(3) Discrepancies between the availability of data and the research described

(4) Inappropriate citations

(5) Incoherent, meaningless and/or irrelevant content included in the article

(6) Peer-review manipulation

The presence of these indicators undermines our confidence in the integrity of the article's content and we cannot, therefore, vouch for its reliability. Please note that this notice is intended solely to alert readers that the content of this article is unreliable. We have not investigated whether authors were aware of or involved in the systematic manipulation of the publication process.

In addition, our investigation has also shown that one or more of the following human-subject reporting requirements has not been met in this article: ethical approval by an Institutional Review Board (IRB) committee or equivalent, patient/participant consent to participate, and/or agreement to publish patient/participant details (where relevant).

Wiley and Hindawi regrets that the usual quality checks did not identify these issues before publication and have since put additional measures in place to safeguard research integrity.

We wish to credit our own Research Integrity and Research Publishing teams and anonymous and named external researchers and research integrity experts for contributing to this investigation.

The corresponding author, as the representative of all authors, has been given the opportunity to register their agreement or disagreement to this retraction. We have kept a record of any response received.

References

[1] M. Liu, Z. Xu, and H. Li, "Effect of Orthodontic Combined with Implant Repair on Aesthetic Effect and Gingival Crevicular Fluid Factor in Patients with Dentition Defect and Periodontitis," *BioMed Research International*, vol. 2022, Article ID 8065313, 12 pages, 2022.

Research Article

Effect of Orthodontic Combined with Implant Repair on Aesthetic Effect and Gingival Crevicular Fluid Factor in Patients with Dentition Defect and Periodontitis

Min Liu,[1] **Zhengmao Xu,**[1] **and Hao Li** ⓘ [2]

[1]*Department of Stomatology, Wuhan Fourth Hospital, Wuhan, Hubei, China*
[2]*Department of Stomatology, Wuhan Hankou Hospital, Wuhan, Hubei, China*

Correspondence should be addressed to Hao Li; 171847232@masu.edu.cn

In order to solve the effect of orthodontics combined with implant repair on the aesthetic effect and gingival crevicular fluid factor of patients with dentition defect and periodontitis, 60 patients who met the diagnostic criteria of chronic periodontitis were proposed. They were randomly divided into treatment group (taking Bushen Huoxue Guchi recipe for 3 courses while basic periodontal treatment) and control group (only basic periodontal treatment without taking any drugs). The experimental method of 30 cases in each group showed that PD, Al, and GI in the treatment group and control group decreased to varying degrees compared with those before treatment. The treatment group decreased significantly compared with the control group ($P < 0.01$). Chronic periodontitis is a common clinical periodontal disease, accounting for up to 95%, local stimulation, a variety of anaerobic bacteria infection, and periodontal plaque, and other factors may cause the occurrence of diseases. Routine treatment mainly includes upper gingival cleaning, lower curettage treatment, and equal root surface treatment. Although the clinical symptoms can be alleviated to a certain extent, the cause cannot be fundamentally excluded, leading to the disease progression in some patients and the formation of aggressive periodontitis and necrotizing periodontal disease.

1. Introduction

Periodontitis is an infectious disease occurring in periodontal tissue, which seriously endangers human oral health. It is one of the important causes of tooth loss, as shown in Figure 1. The third national oral health epidemic survey shows that 80%~97% of adults in China have periodontal problems, and the degree and prevalence of lesions are much higher than those in developed countries [1]. China has gradually entered an aging society, and periodontitis has become the focus of attention. Subgingival scaling and root planning (SRP) is the most important basic periodontal treatment, and it is also the first choice for the treatment of chronic periodontitis. However, mechanical SRP requires high clinical technology. Repeated root leveling and excessive mechanical force can easily to cause root tissue damage, resulting in dentin allergy and root fracture. There are also limitations in the treatment of some special anatomical sites.

Adjuvant treatment with drugs often increases bacterial resistance in patients. Other studies have shown that after mechanical SRP and ultrasonic curettage, the smear layer formed on the root surface may hinder the new attachment of cells to the root surface, which is not conducive to the healing of periodontal tissue [2]. In recent years, with the deepening of laser research in the oral cavity, domestic and foreign scholars have used laser therapy in periodontal treatment. The commonly used lasers include Er: YAG laser and semiconductor laser, which have achieved certain therapeutic effects. Laser has different principles and advantages because of its different wavelengths. Er: YAG laser has good water absorption, removes dental calculus and bone tissue, has little irritation to surrounding tissues and has the potential to kill periodontal pathogens. Clinical reports have also proved that Er: YAG laser can achieve its expected effectiveness and safety in conventional mechanical debridement [2]. In recent years, studies have also found that semiconductor
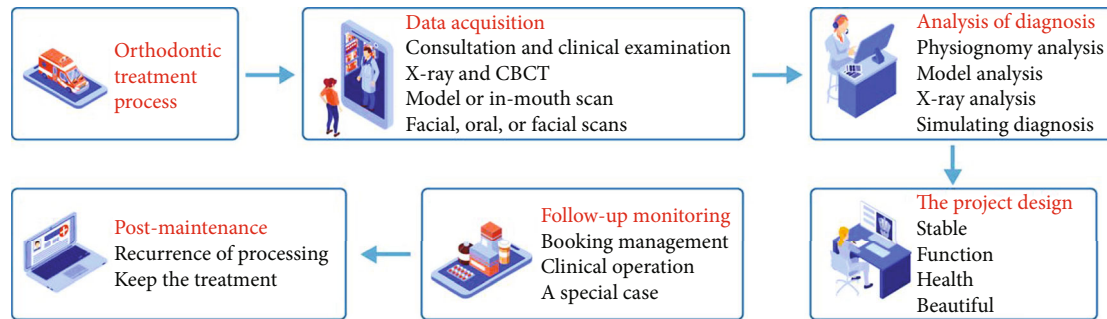
FIGURE 1: Orthodontic treatment process.

laser has the highest absorption rate of hemoglobin, can play the best performance in the environment with blood, has better sterilization, hemostasis, removes granulation tissue, promotes the growth of collagen tissue, and stimulates the repair of periodontal tissue. Because the dose and irradiation mode of laser used in periodontal treatment are different, different treatment parameters also lead to the difference of treatment effect. The study found that single wavelength laser in periodontal basic treatment cannot act on periodontal soft and hard tissues at the same time and the effect on periodontal reattachment after laser treatment, so it cannot achieve the ideal treatment effect. Therefore, different wavelengths of laser are combined to give full play to their respective advantages in order to obtain better periodontal treatment effect. This experiment intends to use the above two commonly used lasers with different wavelengths (semiconductor laser and Er: YAG laser) to treat chronic periodontitis. Divided into three parts, the experiment evaluated the efficacy of dual wavelength laser in the treatment of chronic periodontitis by observing the clinical indexes (PD, BOP, Cal), the content of Pg in subgingival plaque relative to total bacteria and the changes of TNF-α, IL-1β, b-FGF, and TGF-β in gingival crevicular fluid so as to provide a new treatment mode for clinical laser treatment of periodontitis [3].

2. Literature Review

Ma et al. found that periodontal disease is one of the most common oral diseases and is a chronic progressive disease caused by a variety of factors [4]. Due to the reduction of periodontal supporting tissue, patients with periodontal disease are often accompanied by malocclusion deformities such as inclination, displacement, fan-shaped drift, and deep coverage of upper anterior teeth, which is also the initial motivation of most patients for orthodontic treatment. Mikheev et al. believe that orthodontic treatment is a very effective adjuvant treatment for periodontal disease [5]. Qi et al.'s studies on orthodontic treatment of periodontal disease show that after orthodontic treatment, the periodontal condition of patients is significantly improved, the periodontal pocket becomes shallow, the gingivitis is reduced, the tooth stability is increased, and the beauty and function of patients are greatly improved. Self-locking bracket appliance has many advantages in simple operation, time-saving and

labor-saving, low friction, and so on. It has been favored by orthodontists in recent years, but it is unclear whether it is more conducive to the periodontal health of patients with periodontal disease [6]. Sami et al. found that the current research on periodontal status during orthodontic treatment of periodontal disease is mostly about periodontal clinical indicators and plaque index, and there is relatively little about inflammatory factors [7]. Implant denture restoration is called the third set of human teeth because its biomechanical distribution is very close to natural teeth. With the improvement of its technology, it has the advantages of beauty, comfort, stability and no need to grind adjacent teeth. In particular, with the rapid development of guided bone regeneration (GBR), guided tissue regeneration (GTR) and bone cleavage, the scope of implant application has been further expanded. Studies by Hong et al. have shown that the 5-year survival rate of implant restoration of single tooth loss is 93.6%. Such a high retention rate has also become the first choice for more and more patients with chronic periodontitis and one of the main methods to repair dentition loss and dentition defect [8]. Cheng and Zheng found that although implant teeth have many advantages, they are very different from natural teeth in anatomical structure. Implant teeth have no periodontal ligament. Therefore, the "feeling" of implants is much slower than that of natural teeth, and the defense barrier of soft tissue around implants is relatively weak. Once inflammation occurs, bone resorption is more likely to occur, which is likely to make implants loose and fall off due to coinfection [9]. Peri-implant inflammation is the main reason for implant failure and implant fall off. Peri-implantinitis is an inflammatory reaction in the soft and hard tissues around the implant due to the invasion of bacteria and other pathogens. Peri-implant mucositis occurs in mild cases, including increased gingival crevicular fluid, redness and swelling of soft tissue mucosa, exploratory bleeding, and even peri-implant pus. In severe cases, the attachment of implant bone interface is lost, bone tissue is absorbed, and implant is loose, resulting in implant failure. Both of them are bacterial infectious diseases, and their surrounding microbes and clinical manifestations are similar. Studies have shown that the biggest risk factor of peri-implant inflammation may be periodontitis. Torres et al. believe that implant patients with a history of periodontitis have a higher risk of peri-implant inflammation, more prone to peri-implant bone resorption and

greater risk factors of implant failure than implant patients without a history of periodontitis [10]. Zhao et al. believe that there is no direct relationship between periodontitis and peri-implant inflammation. So whether periodontitis patients can receive implant treatment, whether it affects the choice of implant restoration, whether they can obtain a higher implant success rate as periodontal healthy people, or whether such medical history is a potential risk factor for implant failure is still the focus of controversy among many scholars and clinicians [11]. Peri-implantable crevicular fluid (PICF) and natural gingival crevicular fluid (GCF) are the only fluids that directly exude from body fluids. Gorgun et al. found that finding the markers of implant and periodontitis activity from the host reaction products of PICF and GCF is an important aspect of studying peri-implant inflammation [12]. Poormoradi et al. found gingivitis fluid levels were higher in patients with peri-implant edema than in patients with healthy implants, with higher concentrations of inflammatory cytokines in the gingival fluid. Therefore, a quantitative and effective evaluation of scar tissue can be used to measure the health of the tissue around the implant, as well as the treatment effect, which is beneficial to the protection and treatment of crops and flowering plants. Organization [13].

All-porcelain veneers restoration is a new method of cosmetic teeth. Less incisor tissue can be retained from the tooth tissue to the maximum extent. Using adhesive technology to attach porcelain restorative materials over the surface of the tooth can effectively restore the normal shape and color of the tooth.

3. Method

With the rapid development of computer software and hardware technology, image acquisition and processing technology, and 3D digital imaging technology, computer technology has become more and more widely used in orthodontics. We are also facing the digital revolution, especially 3D digital imaging and measurement, as an orthodontic research topic, studying the growth and development of 3D structures of teeth, jaws, face and skull, and malocclusion of various causes. Technology is increasingly used in orthodontic diagnosis, design, treatment, and outcome prediction. The invisible orthodontic technique without brackets achieves the purpose of correction by wearing a series of transparent invisible appliances with certain displacement difference from the teeth on the corrected dentition. The appliance will produce elastic force (orthodontic force) to move the teeth to the predesigned position, and finally move the teeth. The invisible orthodontic technology without brackets mainly includes three-dimensional digital reconstruction technology of dental model, computer-aided design technology of orthodontic process, and manufacturing technology of invisible appliance based on rapid prototyping technology. The efficiency of 3D digital reconstruction technology of dental model directly determines the effect of subsequent correction [14]. Due to the complexity of tooth model morphology, such as shape differences between teeth, and overcrowding between teeth

and missing teeth, the point cloud data has complex details and topology. Based on the background of computer-aided orthodontics, this work proposes a surface reconstruction algorithm and region development based on Delaunay triangulation, which can best solve the problem of reconstructing 3D dental point cloud models [15].

A scattered point cloud reconstruction method based on the combination of Gabriel graph and region growth is proposed. Firstly, the Delaunay triangulation of the sampling point set is calculated to obtain the Gabriel graph of the point set, and then the triangular mesh surface is "grown" by the region growth algorithm. The growth process is to initialize a triangle as the initial region, and then iteratively add new triangular patches only on the boundary edge of the region, so that the region generated in the iterative process will continue to expand [16]. Compared with the traditional region growth algorithm, the algorithm in this paper uses the user-defined acceptability factor as the standard to judge the addition of new triangular patches in the process of region growth, avoids narrow and long triangles to a certain extent, and improves the mesh quality.

STL file is obtained by triangulating and discretizing the CAD solid or surface model. It is equivalent to approximating the CAD model with a polyhedron composed of spatial triangles [17]. The vertices, edges, and faces of the model represented by this file need to meet certain correctness conditions. If the model represented by STL file is regarded as a polyhedron, you can find the relationship between the number of vertices V, the number of edges F, and the number of triangles f in the STL file. The formula is shown in:

$$V + F - E = 2 - 2H, \tag{1}$$

where H represents the number of holes penetrating the body. For a complete STL model, there is no hole penetration so its Euler formula becomes as shown in:

$$F - E + V = 2. \tag{2}$$

In the STL file, each triangle records three edges so that each edge is recorded by the triangle and its adjacent triangles sharing the edge, that is, each edge is recorded twice. Therefore, the relationship between the number of solid edges F and triangle F is shown in:

$$E = 1.5F. \tag{3}$$

Therefore, it is further concluded that the relationship between the number of vertices and triangles is shown in:

$$V = F - F + 2 = 0.5F + 2. \tag{4}$$

Therefore, the STL file has about half the number of vertices and 1.5 times the number of triangles. At the same time, it can be seen from the file format analysis that the correct entity data model described by it must meet the following rules:

Rule 1. Common vertex rule. Each triangle plane must share two vertices with each adjacent small triangle plane,
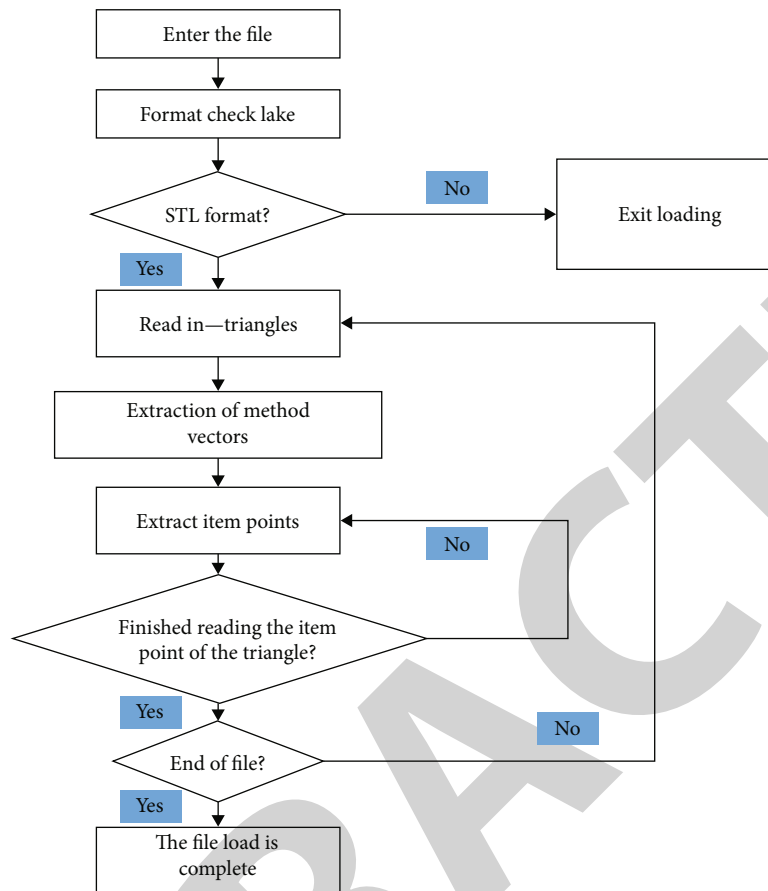
Figure 2: STL file loading.

that is, the vertices of the triangular planes cannot fall on the sides of the adjacent small triangular planes [18]

Rule 2. Orientation rules. The normal vector direction of the triangle plane and the arrangement order of its three vertices conform to the right-hand rule. In other words, the normal direction of each triangle plane corresponds to the order of its three vertices to distinguish the interior and exterior of the represented entity

Rule 3. There are many rules. All surfaces of the 3D model should be covered with a small, leak-free triangular patch

Rule 4. Value rule. The plane vertex coordinates of each small triangle must be positive, while zero and negative values are incorrect. That is, the STL entity should be in the first quadrant (this rule is not necessary. It can be ensured by moving the model to the first quadrant through translation during design)

Read the three vertex coordinate values of each triangular patch in turn to the triangular patch vertex coordinate table. Because the external normal vector of triangular patch can be calculated from the coordinate value of three vertices by the right-hand spiral law, the external normal vector cannot be stored to save storage space. The loading process of STL file is shown in Figure 2. The specific algorithm of STL file loading is as follows [19].

The pathogenesis of periodontitis for plaque microorganisms and their products heavily accumulated in the tooth surface and gingival sulcus, leading to gingival inflammation and swelling, pain, including periodontal support tissue long-term inflammatory reaction can extend to the alveolar bone and cementum, form periodontal bags, cause bag wall inflammatory reaction, loose teeth, and chewing weakness. Surgical repair for the treatment of chronic periodontitis has good clinical value, commonly used repair materials types, models, such as light curing composite resin as ultraminiature composite resin filler, repair operation process, fixed time, but also has the characteristics of wide color gamut, easy to shape, natural after polishing color, has a good beauty fixed repair and aesthetic effect.

Format detection because there is a keyword in ASCII format and these keywords are combined according to a certain relationship, if these keywords are searched in the file, you can judge whether it is the ASCII format of STL file from their combination relationship. Read the subsequent small triangles in turn and put them into the buffer unit.

Take out the information of three points from the buffer unit in turn and put it into the data structure of triangular patch.

Because the hole boundaries are all spatial polygons, the direct repair algorithm is very complex. The spatial polygon can be planarized by projection (Figure 3) so as to reduce the difficulty of repair. In order to achieve a better hole repair effect, we use the hole boundary vertex to construct a least
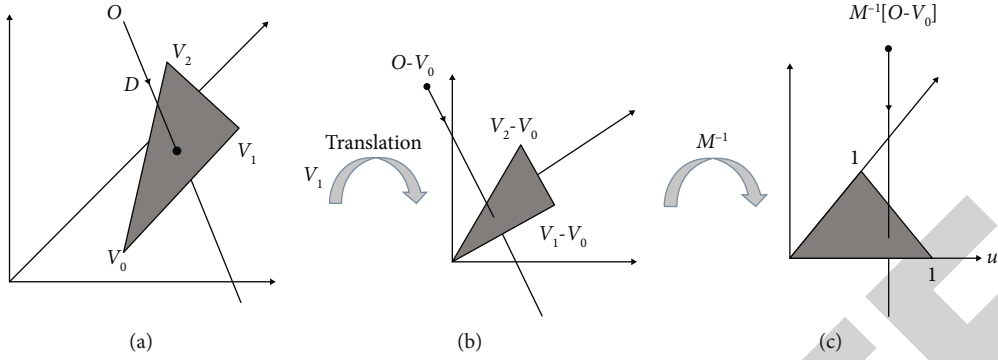
Figure 3: Transformation process.

square surface, and let $p = \{P_i, i = 0, 1, \cdots, n\}$ be the boundary vertex of the hole on the mesh. The least square surface can be determined by the space point O and the normal vector N, where O is the centroid of the space polygon vertex $p_0, p_1, p_2, \cdots p_n$, as shown in

$$O = \frac{1}{n} \sum_{i=1}^{n} p_i. \tag{5}$$

The normal vector N is the unit characteristic corresponding to the minimum eigenvalue of matrix A determined by the following formula:

$$A = \sum_{i=1}^{n} (p_i - o)(pi - o)^T. \tag{6}$$

The projection pi' of the vertex pi of the hole polygon on the feature surface is

$$pi' = pi - \left((pi - o)^T n\right) n. \tag{7}$$

Take the center O of the feature plane as the origin of the new coordinate system, and $P_o - O, Nx(P_o - O), N$ as the x-axis, y-axis, and z-axis of the new coordinate system, respectively. Carry out coordinate transformation on point $pO', p1', p2', \cdots, pi'$, and the z component of point PO', $P1', P2', \cdots, PI'$ after transformation is zero.

The Voronoi diagram and Delaunay triangulation are both classical problems in computational geometry. At present, they have been widely used in the research field of surface reconstruction algorithm, and they are dual to each other [20]. The Voronoi diagram is not only one of the important geometric structures in computational geometry, but also one of the important research contents of computational geometry. Its generation comes from the study of proximity problems. It divides the space into many unit regions according to the nearest attributes of elements in the object set. The point set defined in d-dimensional Euclidean space $p = \{p_1, p_2 \cdots p_n\} \subset R^d, 2 \le d \le \infty, p_i \ne p_j, i \ne j, i, j \in I_n = \{1, 2 \cdots n\}$. The vertical bisector (hyperplane) of segment $p_i p_j$ divides the space (hyperspace) into two

halves, and $H_i(p_i p_j)$ represents the half space on the side of p_i. See the following:

$$V(p_i) = \left\{ xl \|x - p_i\| \le \left\|x - p_j\right\|, j \ne i, j \in I_n \right\} = \cap H_i\left(p_i p_j\right). \tag{8}$$

It is called d-dimensional Voronoi polyhedron about point p_i in R^d space, and set $V(P) = \{V(P_1), V(P_2) \cdots V(P_n)\}$ is called d-dimensional Voronoi graph of point set p. Point p_i is called the growth point of polyhedron $V(P_i)$, also known as the core, and the origin set p is the growth point set of Voronoi diagram $V(P_i)$.

In this region growing algorithm, the correct candidate triangle of a boundary edge is determined by the circumscribed circle radius of the triangle. By selecting the edge with the smallest radius of the circumscribed circle as the candidate edge. However, in the reconstruction of three-dimensional surfaces, this principle is not necessarily applicable. Because the surface to be reconstructed is unknown, there is no certain standard to judge the quality of a reconstructed surface. However, consider a sheet tetrahedron whose four vertices are on a circumscribed sphere. Assuming that the initial triangle of the surface s to be reconstructed is FCD, it is correct in topology and geometry to select any triangle in the tetrahedron as a candidate triangle. However, there is also another case here. If the initial triangle of S is CDA and the radius of the circumscribed circle in the effective triangle of edge e is exactly CDB, this choice is obviously inappropriate. In order to solve this problem, we introduce a constant a_{sliver}. If the dihedral angle between the triangle and S is less than a_{sliver}, we do not consider it a candidate triangle even if its circumscribed circle radius is the smallest.

Assuming that the triangle related to boundary edge $e \in \partial s$ is t and the triangle related to edge e contained in surface s is t_b, we use β_t to represent the absolute value of the angle between the normals between t and t_b, then the candidate triangle c_e of boundary edge $e \in \partial s$. It can be defined as follows, see the following:

$$c_e = \arg \min \{r_t \text{It is valid for } e \text{ and } \beta_t < a_{silver}\}, \tag{9}$$

where r_t represents the circumscribed circle radius of triangle t. a_{sliver} is the constant mentioned above, but its value is not strictly specified.

According to experience, it is usually set to $5\pi/6$. If none of the valid triangles of edge e satisfies the above conditions, the candidate triangle c_e of edge e is empty. After the candidate triangles of boundary edges are determined, the next step is to select one of all candidate triangles and add it to the construction surface s. The heuristic search strategy can better select the appropriate triangle in the fully sampled point cloud model, but when the sampling points are sparse, the strategy will fail. Using greedy algorithm, the candidate triangle with the highest reliability is selected to join the surface s every time, so the focus of the problem is how to judge the reliability of a candidate triangle. According to the triangle related to edge e is t_b and the dihedral angle β_t between it and the candidate triangle, the smaller β_t is, the higher the reliability of the triangle is and the more likely it is to be added to s. In other words, the smoother the local surface s is, the more reliable the candidate triangle is. On this basis, this paper proposes a concept of local smoothness degree (LSD) and applies it to regional growth to judge the reliability of a candidate triangle. LSD is defined as follows: assuming that nt_i is the i-th adjacent triangle of triangle t and $\beta(t, nt_i)$ represents the dihedral angle between them, see the following:

$$\text{LSD}(t) = \underline{1} \overset{n}{\Sigma} \cos(\beta(\text{t}, \text{nt}_i)), \tag{10}$$

where n represents the number of adjacent triangles of t. In this algorithm, it specifically refers to the number of adjacent candidate triangles, so it has $1 \le n \le 3$. From the definition of LSD, we can see that the larger the LSD value of a candidate triangle, it means that it can make the generated surface s smoother locally, and the greater the reliability of the candidate triangle relative to the one with small LSD value.

When the local smoothness LSD values of two candidate triangles are large, it is not very appropriate to use only the LSD value to judge the reliability of candidate triangles, especially when the surface is noisy. Because these two candidate triangles can make the generated surface locally smooth, at this time, we can judge their reliability by comparing the circumscribed circle radius of the two candidate triangles. The one with small circumscribed circle radius has higher reliability. When the algorithm is executed, the candidate triangles with high reliability are preferentially added to the surface S through a priority queue. When candidate triangles $t \ne \varnothing$, its priority $p(t)$ can be defined as follows, as shown in the following:

$$p(t) \begin{cases} 1/r_t \\ LSD(t) = \dfrac{1}{n} \sum_{i=1}^{n} \cos(\beta(t, nt_i)) \end{cases}. \tag{11}$$

Among them, a is a preset constant threshold, and there is no constant value. According to the test results, $a = \sqrt{3/2}$ is usually selected. When the value of LSD (t) is greater than

a, the dihedral angle between adjacent triangular patches is less than 30° on average, which can meet most of the requirements of local fairing. When the candidate triangle $t \ne \Phi$, its priority $p(t) = -\infty$.

Picking operation plays a basic role in 3D interactive program. It is the operation to locate the object in the screen and determine the selected object. The basic principle of feature point picking is to find the point closest to the observer in the intersection of the observation line passing through the mouse position point and the mesh model, that is, the surface point picking operation is actually the intersection calculation operation. Without losing generality, the model considered in this paper is triangular mesh model (polygon model can be transformed into triangular mesh model through plane triangulation), and its pickup process is the intersection calculation of ray and triangle. The ray $R(t)$ parameter equation with starting point o and unit direction vector D is shown in the following:

$$R(t) = O + tD. \tag{12}$$

The three vertices are triangles with V_0, V_1, V_2, respectively, and the coordinates of its internal point $P(u, v)$ are shown in the following:

$$p(u, v) = (1 - u - v)V_0 + uV_1 + vV_2. \tag{13}$$

Calculating the intersection of ray $R(t)$ and triangle is equivalent to equation (0.1), see the following:

$$[-D \; V_1 - V_0 \; V_2 - V_0]u = O - V_0. \tag{14}$$

Geometrically, the above equation can be regarded as translating the triangle to the coordinate origin and transforming it into a unit triangle located in the oyz plane. Its transformation matrix is $M = [-D \; V_1 - V_0 \; V_2 - V_0]$. At this time, the direction of the ray is adjusted to the x-axis, and its transformation process is shown in the transformation process of Figure 3 [21].

4. Experiment and Discussion

60 patients with chronic periodontitis in the outpatient department of Stomatology of a Provincial Traditional Chinese Medicine Hospital from March 2020 to October 2020 were selected and agreed to participate in this study and sign the informed consent form [22]. According to the diagnostic criteria of chronic periodontitis proposed by the American Symposium on Classification of Periodontal Diseases in 1999, each patient underwent systematic periodontal examination. The patients have no systemic diseases, smoking history, pregnancy, immunosuppressants, nonsteroidal anti-inflammatory drugs, and hormone drugs in the recent 3 months, and they have not received periodontal treatment in the recent 6 months. Each patient has at least 20 natural teeth in the mouth and at least 2 tooth positions in each quadrant. The inclusion criteria are as follows: (1) there is no caries and filling in the tooth neck; (2) Gingival index > 1, periodontal probing depth $\ge 4\,\text{mm}$, and attachment

Table 1: Instruments and apparatus.

Instrument	Company
Ultrasonic scaler	EMS, Switzerland
Manual curette	Shanghai Stomatological Medical Equipment Factory
Sampling gun	Biohit, Finland
Micro compounder	WH2, Shanghai ChuDing Analytical Instrument Co., Ltd
Pipette	Rainin, USA
Electronic analytical balance	Shanghai YIDA Medical Instruments Co., Ltd.
Ultra low temperature freezer	Zhongke Meiling
Freezing centrifuge	Beijing Baiyang Medical Equipment Co., Ltd.
Automatic microplate reader	Thermo EI ECTRON
Flush syringe	CORPORATION
Filter paper strip	Shandong Weigao Group Medical Polymer Co., Ltd.
EP tube	Fushun civil affairs filter paper factory
Periodontal probe	Eppendorf, Germany

Table 2: Reagents.

Reagent name	Batch number	Manufacturer
Human interleukin-1β ELISA kit	1101B6053	Hangzhou Lianke Biotechnology Co., Ltd
Human tumor necrosis factor-a ELISA kit	118260921	Hangzhou Lianke Biotechnology Co., Ltd
Human matrix metalloproteinase-2 ELISA kit	11M0260947	Hangzhou Lianke Biotechnology Co., Ltd
3% hydrogen peroxide solution	0059	Shandong Lierkang Medical Technology Co., Ltd.
PBS buffer	8116104	Shanghai Lifei Biotechnology Co., Ltd.

loss ≥ 2 mm; (3) X-ray film showed that the horizontal absorption of alveolar bone did not exceed 1/2 of root length; and (4) the looseness of affected teeth is less than grade II. See Table 1 for instruments and apparatus.

Reagent details are shown in Table 2.

60 cases had onset for 7 to 10 years, including 28 males and 32 females. Patients were 43-62 years old. 60 patients who met the criteria were divided into treatment group and management group, 30 cases in each group. Group 3 had shifts of Bushen Huoxue Guchi Formula (7 days per shift) combined with traditional treatment. During the first 7-9 years, the outbreak appears to have intensified, averaging 8.27 + 0.69.There were 13 men and 17 women. The minimum age was 43 years, the maximum age was 61 years, and the average age was 51.63 + 4.00 years. The control group had only treatment and generally no medication. Life expectancy is 8-10 years, with an average of 8.60 ± 0.67. There are 15 men and 15 women. The youngest was 46 years old, the oldest was 62 years old, and the median age was 52.47 ± 3.29 years [23]. After analysis, there were no significant differences in age, gender, disease, etc. between the two groups, as shown in Table 3 ($P > 0.05$). This is equivalent.

Periodontitis is a common periodontal chronic infectious disease in China, which usually causes damage to the periodontal supporting tissues such as the gingiva, periodontal membrane, and alveolar bone. Tooth loosening, defect, displacement, and elongation are common clinical manifestations of periodontitis, and severe cases can lead to the appearance of periodontal malalignment deformity and cause occlusal trauma, with a serious impact on the health of periodontal tissue.

The treatment plan of periodontitis is to eliminate local irritants and control plaque first, and then carry out follow-up treatment after the local inflammation is basically eliminated. After one week of basic periodontal treatment, the symptoms of gingivitis and the content of inflammatory factors in gingival crevicular fluid were relatively stable. At this time, the periodontal status was taken as the baseline level of this experiment. The periodontal status-related indexes of the tested teeth were examined and recorded in the two groups, and the gingival crevicular fluid was collected at the same time [24]. The treatment group took Bushen Huoxue Guchi recipe for 3 courses. After 4 weeks of basic treatment in the control group, the periodontal status-related indexes of the examined teeth and gingival crevicular fluid were checked and recorded again at the same time. Basic periodontal treatment was as follows: (1) plaque control: the number of dental surfaces with plaque shall be

TABLE 3: Comparison of gender, age, and course of disease between the treatment group and control group ($n = 30$).

Group	Gender [male (%)]	Age (years) (xs)	Course of disease (year) ($+ s$)
Treatment group	[12 (43%)]	51.53 ± 4.08	8.57 ± 0.63
Control group	[15 (80%)]	56.47 ± 3.99	8.67 ± 0.66
P	0.785 ∗	0.325 ∗	0.068 ∗

TABLE 4: Comparison of GI between the treatment group and control group after 4 weeks of basic treatment ($n = 30$).

Group/GI score	0	1	2	3
Treatment group (number of cases)	1	18	10	1
Control group (number of cases)	0	11	20	0

controlled below 20% of the total number of dental surfaces examined; (2) supragingival scaling: ultrasonic scaler was used to remove plaque, supragingival calculus, and pigmentation and polish the tooth surface; (3) subgingival curettage: the subgingival curettage device was used to scrape the calculus and plaque on the root surface in the periodontal pocket; (4) occlusal adjustment to establish a balanced occlusal relationship; and (5) oral education.

In the treatment group, one week after basic periodontal treatment, oral Bushen Huoxue Guchi formula, one dose per day, conventional decoction, 300 ml juice, oral twice in the morning and evening, every 7 days as a course of treatment, a total of 3 courses of treatment. Oral hygiene examination shall be conducted once a week to ensure good oral hygiene [25].

In the control group, only basic periodontal treatment without taking any drugs. Oral hygiene examination was conducted once a week to ensure good oral hygiene.

One test tooth (preferably the right lower first molar; if the right lower first molar is missing, choose either the left lower first molar or the right lower first molar) for each patient. Six sites of each tested tooth (oral mesial, middle and distal, lingual mesial, middle, and distal) were selected to identify and record indicators related to periodontal condition (GI, PD, and Al). At the same time, the gingival crevicular fluid was collected to detect the concentrations of IL-1β, TNF-α, and MMP-2 in the gingival crevicular fluid. The tooth positions of the tested teeth were consistent before and after the experiment. Dry the gums of the tested teeth, place a periodontal probe 0.5-1 mm below the gingival margin, and observe the bleeding after light scraping. The buccal and supralingual papillary areas were divided into four papillary areas, and the buccal and supralingual papillary areas were recorded as papillary areas. Grading standard was as follows: 0 = normal gums; 1 = mild gingival inflammation: slight color change, mild edema, and no bleeding after probing; 2 = moderate gingival inflammation: red, edematous, bright, probing bleeding; 3 = severe gingival inflammation: obvious redness and edema, or ulcer, with spontaneous bleeding tendency. The loss of attachment is the distance from the bottom of the periodontal pocket to the enamel cementum boundary. When the periodontal pocket is formed and the PD exceeds 3 mm, the tooth junction epithe-

lium shifts to the root and the periodontal supporting tissue is damaged, the loss of attachment occurs. Gingivitis and periodontitis are 0. Periodontal probe with Williams scale, in mm, rounded. When there is no gingival retraction: loss of attachment = depth of periodontal probing-distance from enamel cementum boundary to gingival margin. During gingival recession: loss of attachment = periodontal probing depth + distance from enamel cementum boundary to gingival margin. Measure, calculate and record six parts of each tested tooth: lingual mesial, central, distal and buccal mesial, central, and distal. The average values of the six parts are compared and analyzed as the loss of periodontal attachment for statistical processing, as shown in Tables 3–7 and Figure 4.

One test tooth (preferably the right lower first molar, if the right lower first molar is missing, the left lower first molar or the right lower second molar) is taken from each patient. Each tested tooth selects 6 sites (buccal near middle, middle and far middle, lingual near middle, middle, and far middle) to check and record the periodontal status related indicators (GI, PD, and Al) and collect gingival crevicular fluid to detect the concentration of MMP-2 in gingival crevicular fluid. The tooth position of the tested teeth was consistent before and after the experiment. Blow dry the gingiva of the tested teeth, place the periodontal probe 0.5~1 mm below the gingival margin, and observe whether there is bleeding after gently scratching [26]. Divide the gingival papilla area above the buccal and lingual sides into 4 gingival papilla areas, and record the gingival papilla area above the buccal and lingual sides as gingival papilla areas. Grading standard was as follows: 0 = normal gums; 1 = mild gingival inflammation: slight color change, mild edema and no bleeding after probing; 2 = moderate gingival inflammation: red, edematous, bright, probing bleeding; 3 = severe gingival inflammation: obvious redness and edema, or ulcer, with spontaneous bleeding tendency. The loss of attachment is the distance from the bottom of the periodontal pocket to the enamel cementum boundary. When the periodontal pocket is formed and the PD exceeds 3 mm, the tooth junction epithelium shifts to the root and the periodontal supporting tissue is damaged, and the loss of attachment occurs. Gingivitis and periodontitis are 0. Periodontal probe with Williams scale, in mm, rounded. When there is no

Table 5: Comparison of Al between treatment group and control group ($x + s$) ($n = 30$).

Group/time	1 week	4 weeks	F	P
Treatment group	2.97 ± 0.72	1.47 ± 0.67	53.254 ***	<0.001 ***
Control group	3.17 ± 0.78	2.45 ± 0.68	20.905 ****	<0.002 ****
F	1.235 *	2.87.69 **	—	—
P	0.259 *	<0.002 **	—	—

Table 6: IL-1 in the treatment group and control group β Comparison of (PG/ml) ($x + s$) ($n = 30$).

Group/time	1 week	4 weeks	F	P
Treatment group	694.09 ± 56.98	275.60 ± 42.09	653.97 **	<0.001 ***
Control group	657.60 ± 60.48	374.79 ± 49.77	338.895 ***	<0.001 ****
F	0.161 *	635.89 **	—	—
P	0.977 *	<0.001 **	—	—

Table 7: Comparison of MMP-2 between the treatment group and control group (PG / ml) ($x + s$) ($n = 30$).

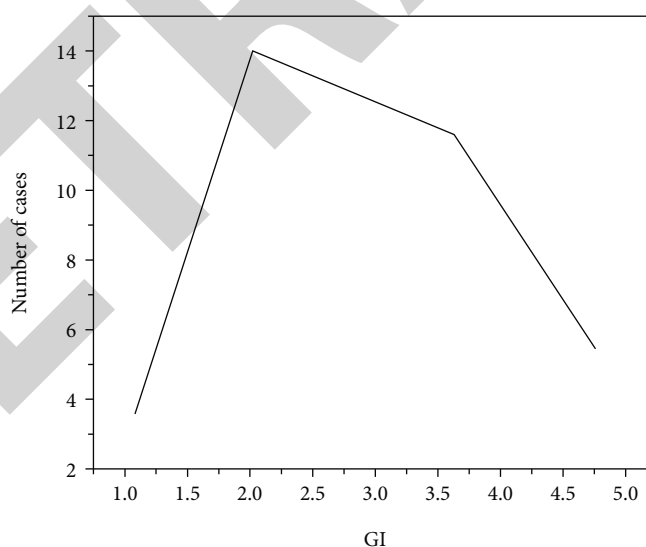| Group / time	1 week	4 weeks	F	P
Treatment group	139.21 ± 28.17	64.96 ± 20.46	154.076 ***	<0.001 ***
Control group	129.31 ± 24.93	87.87 ± 15.43	54.778 ****	<0.001 ****
F	0.187 *	916.978 **	—	—
P	0.658 *	<0.001 ***	—	—

Figure 4: Comparison of GI at baseline between the treatment group and control group.

gingival retraction: loss of attachment = depth of periodontal probing-distance from enamel cementum boundary to gingival margin; During gingival recession: loss of attachment = periodontal probing depth + distance from enamel cementum boundary to gingival margin. Measure, calculate, and record six parts of each tested tooth: lingual mesial, central, distal and buccal mesial, central, and distal. The average values of the six parts are compared and analyzed as the loss of periodontal attachment for statistical processing, as shown in Tables 3–7 and Figure 4 [27].

Periodontitis is a chronic destructive tissue disease. Notable symptoms of treatment are gingival swelling, periodontal pocket formation, alveolar bone resorption, and tooth loosening. Periodontitis not only leads to premature tooth loss in adults but also induces various systemic diseases, which seriously affects the physical and mental health

of patients. In addition to the direct role of suspected periodontal pathogens in destroying periodontal tissue, the host response to periodontal pathogens includes the recruitment of immune cells and immune-related cells and their subsequent release of inflammatory factors (cytokines and various enzymes), which play an important role in the pathological process of periodontal disease. The extraction of periodontitis marker inflammatory factors from gingival crevicular fluid (GCF) is a commonly used method to detect periodontitis, and has become a hot spot in the study of periodontitis. GCF is produced through the permeability of gingival sulcus epithelium. Tissue fluid penetrates into gingival tissue from capillaries in subcutaneous connective tissue above gingival sulcus to form intercellular fluid, which is then absorbed through lymphatic reflux. When the amount of exudation is greater than the return flow, the intercellular fluid forms edema or extravasates into gingival sulcus through binding epithelial cell space to form GCFP. In 1959, Brill found the presence of GCF in the V-shaped gingival sulcus formed between the epithelial lining of the free gingiva in the human tooth neck and the teeth and considered GCF as an inflammatory exudate. Gingival crevicular fluid comes from local microcirculation and connective tissue fluid, which contains a variety of chemicals, especially the contents of IL-1β, TNF-α, and MMP-2 reflect the severity of periodontitis. There is only a small amount of GCF in gingiva under physiological conditions. When there is inflammation, the vascular permeability increases, the epithelial space in the sulcus widens, and the amount and composition of GCF also change. The research on the relationship between GCF and periodontal has been widely carried out. With the in-depth study of the pathogenesis of periodontitis, the biological reaction of periodontal tissue in the treatment of periodontitis with traditional Chinese medicine has attracted more and more attention of scholars. Among them, the change of chemical substances in gingival crevicular fluid caused by traditional Chinese medicine has become the focus of scholars' attention. This method has the advantages of noninvasive, simple, and repeatable operation. In this study, the GI of the treatment group before treatment was 0, 0 cases of grade 1, 12 cases of grade 2, and 18 cases of grade 3. After three courses of treatment (3 weeks), the GI was 1 case of grade 0, 18 cases of grade 1, 11 cases of grade 2, and 0 cases of grade 3. In the control group, GI was grade 0, grade 1 in 0 cases, grade 2 in 19 cases, and grade 3 in 11 cases after 1 week of basic treatment, after 4 weeks of basic treatment, there were 0 cases of grade 0, 11 cases of grade 1, 19 cases of grade 2, and 0 cases of grade 3. In the treatment group, mean PD was $6.00 + 0.84$ mm before treatment and $4.60 + 0.92$ mm after treatment. After 1 week of baseline treatment, the mean PD in the control group was $5.62 + 0.89$ mm, which decreased to $4.57 + 0.94$ mm after 4 weeks. The average Al in the treatment group was 2.90 ± 0.78 mm before treatment, and decreased to 1.85 ± 0.65 mm after treatment. The AL in the control group was 3.13 ± 0.68 mm after 1 week of basic treatment, and decreased to 2.30 ± 0.58 mm after 4 weeks. In this experiment, the PD, GI, and AL indexes related to the periodontal condition of the examined teeth in both the treatment group and the control group decreased, and the decrease in the treatment group was more significant than that in the control group $P < 0.01$. The results showed that the effect of basic therapy combined with Bushen Huoxue Guchi recipe on gastrointestinal shrinkage was better than that of the basic therapy group.

5. Conclusion

This work studies the error detection and processing algorithm of the triangular mesh model. Firstly, according to the characteristics of common errors of triangular mesh model are classified. Because the objects processed in this paper are tooth models with a large amount of data, in order to improve the detection speed, the mesh space of the mesh model is divided by using octree data structure before detecting mesh errors, and then various common error triangular mesh detection and processing algorithms are proposed to realize the function of triangular mesh model error detection and processing. MMP-2 is mainly expressed by epidermal cells, fibroblasts, endothelial cells, and osteoclasts. It is secreted as an inactive zymogen of 72 KD with an activated molecular weight of 62 KD. MMP-2, MT1-MMP, and TIMP-2 can form triple complexes within the cell membrane and synergistically act on the proteolysis of activated MMP-2. MMP-2 can activate many cytokines, such as IL-1, transforming growth factor-β, and TNF-α. It plays an important role in regulating acute and chronic inflammation, apoptosis, and chemotaxis of macrophages. Li et al. reported that the expression of MMP-2 in periodontal gingival tissue was significantly higher than that in normal gingival tissue, and the activation of MMP-2 was closely related to the pathogenesis of periodontitis. In this experiment, the average concentration of MMP-2 in gingival fluid before treatment was 136.21 ± 28.19 ng/ml, and the average concentration of MMP-2 in gingival fluid after treatment was $63, 96 \pm 20.47$ ng/ml; one week after the baseline treatment, the average concentration of MMP-2 in the cleft palate fluid of the control group was 124.30 ± 24.94 ng/ml. After 4 weeks, the average concentration of MMP-2 in gingival fluid was 85.25 ± 17.29 ng/ml, and the reduction in the treatment group was significantly greater than that in the control group. The difference between the two groups was statistically significant ($P < 0.01$), indicating that the baseline treatment combined with Bushen Huoxue Guchi had a better effect on reducing the concentration of inflammatory factor MMP-2 than the baseline treatment group.

Data Availability

No data were used to support this study.

Conflicts of Interest

There are no potential competing interests in our paper. And all authors have seen the manuscript and approved to submit to the journal. We confirm that the content of the manuscript has not been published or submitted for publication elsewhere.

Authors' Contributions

Min Liu and Zhengmao Xu contributed equally to this work as co-first author.

References

[1] Y. J. Cui, J. Liu, M. M. Liu, and H. Z. Zhang, "Observation on the clinical effect of apatinib combined with chemotherapy in the treatment of advanced non-small cell lung cancer," *Pakistan Journal of Medical Sciences*, vol. 37, no. 4, pp. 1036–1041, 2021.

[2] M. Harada-Karashima, Y. Ishihara, H. Kamioka, and R. Kanomi, "Age-related changes in the effect of rapid maxillary expansion on the position of labially impacted maxillary canines: a case-control study," *American Journal of Orthodontics and Dentofacial Orthopedics*, vol. 159, no. 3, pp. 305–311, 2021.

[3] Q. Liu, C. Zhou, J. J. Xin, Y. X. Zhao, and X. C. Yu, "Observation on facilitation and attenuation effect of electroacupuncture combined with aconitine for treatment of heart failure in rats," *Zhen ci yan jiu= Acupuncture Research*, vol. 46, no. 7, pp. 570–574, 2021.

[4] Y. H. Ma, G. Liu, and J. Yang, "Observation on the effect of local flap transfer and sclera transplantation in repairing skin defect after eyelid tumor operation," *Nepalese Journal of Cancer*, vol. 4, no. 1, pp. 28–31, 2020.

[5] K. G. Mikheev, R. G. Zonov, D. L. Bulatov, A. E. Fateev, and G. M. Mikheev, "Laser-induced graphene on a polyimide film: observation of the photon drag effect," *Technical Physics Letters*, vol. 46, no. 5, pp. 458–461, 2020.

[6] F. X. Qi, Y. Hu, L. J. Kang, P. Li, and X. Zhang, "Effects of butyphthalide combined with idebenone on inflammatory cytokines and vascular endothelial functions of patients with vascular dementia," *Journal of the College of Physicians and Surgeons Pakistan: JCPSP*, vol. 30, no. 1, pp. 23–27, 2020.

[7] S. S. Cakir, R. B. Degirmentepe, H. A. Atalay et al., "The effect of overactive bladder treatment with anticholinergics on female sexual function in women: a prospective observational study," *International Urology and Nephrology*, vol. 51, no. 1, pp. 27–32, 2020.

[8] H. P. Hong, Y. Tao, C. Zhong, J. Li, and Y. Y. Xu, "Evaluation of therapeutic effects of the ultramicro needle knife combined with cervical spine fine adjusting on youth cervical curvature abnormality case," *Zhongguo gu shang = China Journal of Orthopaedics and Traumatology*, vol. 33, no. 6, pp. 524–529, 2020.

[9] Z. Cheng and W. Zheng, "Clinical effect and aesthetic observation of all-on-4 immediate loading implant denture in severe periodontitis," *Evidence-based Complementary and Alternative Medicine*, vol. 2021, no. 2, Article ID 3120260, 9 pages, 2021.

[10] F. G. Torres, A. Corradini, and E. Sánchez, "Oral rehabilitation and management of the patient with terminal dentition: clinical and laboratory case after 3 years of follow-up," *Current Oral Health Reports*, vol. 8, no. 3, pp. 29–47, 2021.

[11] D. Zhao, A. T. Khawaja, L. Jin et al., "Effect of non-surgical periodontal therapy on renal function in chronic kidney disease patients with periodontitis: a systematic review and meta-analysis of interventional studies," *Clinical Oral Investigations*, vol. 24, no. 4, pp. 1607–1618, 2020.

[12] E. P. Gorgun, H. Toker, A. Tas, A. L. Alpan, and Y. Silig, "Il-13 gene polymorphisms (-1112 c/t and -1512 a/c) in patients with chronic and aggressive periodontitis: effects on GCF and outcome of periodontal therapy," *Nigerian Journal of Clinical Practice*, vol. 24, no. 7, pp. 965–972, 2021.

[13] B. Poormoradi, L. Gholami, R. Fekrazad, A. Hooshyarfard, and M. Farhadian, "Comparison of the effect of Er,Cr:YSGG laser and halita mouthwash on oral malodor in patients with chronic periodontitis: a randomized clinical trial," *Journal of Lasers in Medical Sciences*, vol. 12, no. 1, pp. e26–e26, 2021.

[14] A. Sari, V. Davutoglu, E. Bozkurt, I. L. Taner, and K. Erciyas, "Effect of periodontal disease on oxidative stress markers in patients with atherosclerosis," *Clinical Oral Investigations*, vol. 26, no. 2, pp. 1713–1724, 2022.

[15] N. Ziaei, S. Golmohammadi, M. Ataee, F. Ardalani, and M. M. Abbasi, "Effect of non-surgical periodontal treatment on three salivary adipokines in diabetic patients with periodontitis," *Journal of Dental Research Dental Clinics Dental Prospects*, vol. 14, no. 3, pp. 199–205, 2020.

[16] W. Buwembo, I. G. Munabi, M. Kaddumukasa, H. Kiryowa, and N. K. Sewankambo, "Non-surgical oral hygiene interventions on disease activity of rheumatoid arthritis patients with periodontitis: a randomized controlled trial," *Journal of Dental Research Dental Clinics Dental Prospects*, vol. 14, no. 1, pp. 26–36, 2020.

[17] C. M. Meijndert, G. M. Raghoebar, A. Vissink, and H. Meijer, "Alveolar ridge preservation in defect sockets in the maxillary aesthetic zone followed by single-tooth bone level tapered implants with immediate provisionalization: a 1-year prospective case series," *International Journal of Implant Dentistry*, vol. 7, no. 1, pp. 18-19, 2021.

[18] C. Meijndert, G. Raghoebar, A. Vissink, and H. Meijer, "A prospective clinical study with 60 patients on the performance of a bone level tapered implant in the aesthetic zone," *Clinical Oral Implants Research*, vol. 31, Supplement20, pp. 256–256, 2020.

[19] J. Allan, D. Goltsman, P. Moradi, and J. A. Ascherman, "The effect of operative time on complication profile and length of hospital stay in autologous and implant-based breast reconstruction patients: an analysis of the 2007-2012 ACS-NSQIP database," *Journal of Plastic, Reconstructive & Aesthetic Surgery*, vol. 73, no. 7, pp. 1292–1298, 2020.

[20] M. Nabarrette, J. Brunheroto, P. R. Dos Santos, M. D. C. Meneghim, and S. A. Vedovello, "Esthetic impact of malocclusions in the anterior segment on children in the mixed dentition," *American Journal of Orthodontics and Dentofacial Orthopedics*, vol. 159, no. 1, pp. 53–58, 2021.

[21] B. Y. Park, S. E. Hong, M. K. Hong, and K. J. Woo, "The influence of contralateral breast augmentation on the development of complications in direct-to-implant breast reconstruction," *Journal of Plastic, Reconstructive & Aesthetic Surgery*, vol. 73, no. 7, pp. 1268–1276, 2020.

[22] B. Atiyeh and S. Emsieh, "Breast implant illness (BII): real syndrome or a social media phenomenon? A narrative review of the literature," *Aesthetic Plastic Surgery*, vol. 46, no. 1, pp. 43–57, 2021.

[23] L. E. Carneiro-Campos, L. B. Freitas-Fernandes, D. Masterson et al., "Does the natural maxillary dentition influence the survival rate of mandibular metal-resin implant-supported fixed complete dentures? A systematic review and meta-analysis," *The Journal of Prosthetic Dentistry*, vol. 124, no. 1, pp. 36–45, 2020.

[24] J. M. Alberga, K. Stellingsma, H. Meijer, H. A. Oostenbrink, A. Vissink, and G. M. Raghoebar, "Dental implant placement in alveolar cleft patients: a retrospective comparative study on clinical and aesthetic outcomes," *International Journal of Oral and Maxillofacial Surgery*, vol. 49, no. 7, pp. 952–959, 2020.

[25] I. Sarfati, J. Millochau, I. Meredith et al., "Salvaging the infected breast implant: results of a retrospective series of 80 consecutive cases," *Journal of Plastic, Reconstructive & Aesthetic Surgery*, vol. 73, no. 12, pp. 2232–2238, 2020.

[26] S. H. Low, S. L. Lu, and H. K. Lu, "Evidence-based clinical decision making for the management of patients with periodontal osseous defect after impacted third molar extraction: a systematic review and meta-analysis," *Journal of Dental Sciences*, vol. 16, no. 1, pp. 71–84, 2021.

[27] F. L. Mendonça, C. C. L. Di Leone, I. C. Grizzo et al., "Simplified occlusal replica adapted technique with glass ionomer cement for molar-incisor hypomineralization-affected molars: An 18-month follow-up," *Journal of the American Dental Association (1939)*, vol. 151, no. 9, pp. 678–683, 2020.